

# Quantum Decoherence in Superconducting Circuits: Contrasting Loss Mechanisms of Nb and Si Surface Oxides

**D. Frank Ogletree,<sup>1†</sup> Virginia Altoé,<sup>2</sup> Adam Schwartzberg,<sup>2</sup> Chengyu Song,<sup>1</sup> David I. Santiago,<sup>2</sup> Irfan Siddiqi<sup>3</sup>**

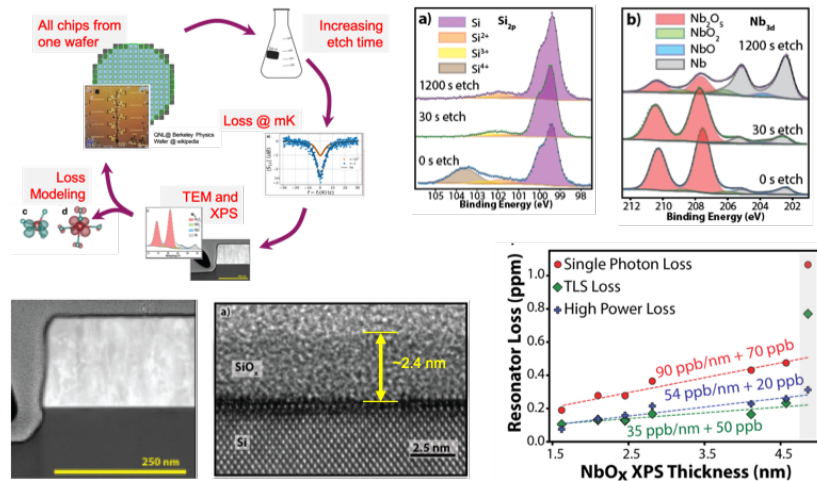
<sup>1</sup> *Molecular Foundry Division, Lawrence Berkeley Lab, Berkeley CA 94720 USA*

<sup>2</sup> *Computing Sciences, Lawrence Berkeley Lab, Berkeley CA 94720 USA*

<sup>3</sup> *Physics Department, University of California, Berkeley CA 94720 USA and  
Materials Sciences Division, Lawrence Berkeley Lab, Berkeley CA 94720 USA*

The performance of quantum sensors or qubits based on superconducting circuits is limited by “two level system” (TLS) loss associated with amorphous layers at the metal and substrate interfaces [1,2]. Through selective chemical etching of niobium-on-silicon quantum resonators, correlated with millikelvin microwave loss measurements and interfacial materials analysis [3], we found clear differences in contributions of Si and Nb surface oxides. XPS and STEM analysis of resonator cross-sections were used to correlate physical and chemical changes in the surface oxides with reductions in decoherence [4,5]. Surface SiO<sub>x</sub> hosted 70% of TLS loss, with only 24% associated with NbO<sub>x</sub>. Although TLS loss dominated decoherence, 39% of loss did not show the characteristic TLS power dependence [1]. NbO<sub>x</sub> hosted 68% of non-TLS losses, with only 17% associated with SiO<sub>x</sub>. We localized 92% of all loss in the surface oxides. TEM diffraction showed an epitaxial relation between the Nb superconducting film and the Si substrate, with no evidence for the commonly-reported metal-substrate amorphous oxide layer. Post-fabrication surface oxide etching improved our median quantum-resonator quality factors from 0.93 to 5.26 million.

**Figure 1.** Experiment scheme (top left); XPS of etched Si and Nb oxides (top right); STEM images of Nb film and Si surface oxide (bottom left); Correlation of losses with oxide thickness (bottom right)



[1] Müller et al, ‘Towards understanding two-level-systems in amorphous solids: insights from quantum circuits’, *Rep Prog Phys*, 2019.

[2] Siddiqi, ‘Engineering high-coherence superconducting qubits’, *Nat Rev Mat*, 2021

[3] Altoé et al, ‘Localization and mitigation of loss in niobium superconducting circuits’ *PRX Quantum*, 2022.

[4] Sheridan et al, ‘Microscopic Theory of Magnetic Disorder-Induced Decoherence in Superconducting Nb Films’, *arXiv* 2111.11684, 2021.

[5] Harrelson et al, ‘Elucidating the local atomic and electronic structure of amorphous oxidized superconducting niobium films’, *App Phys Lett* 2021.

† Author for correspondence [dfogletree@lbl.gov](mailto:dfogletree@lbl.gov)

# Supplemental Information

## 1) Details of Microwave Resonator Characterization

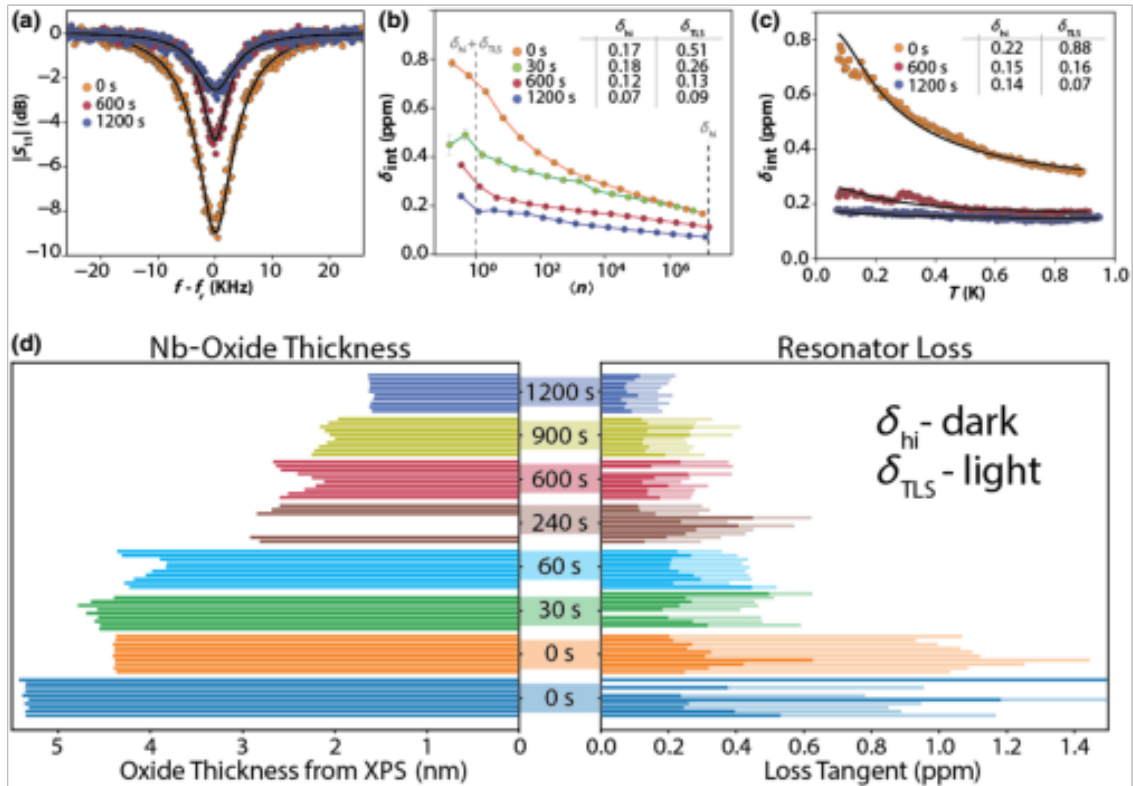
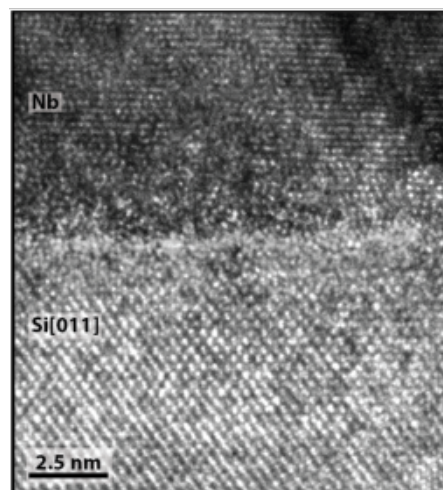
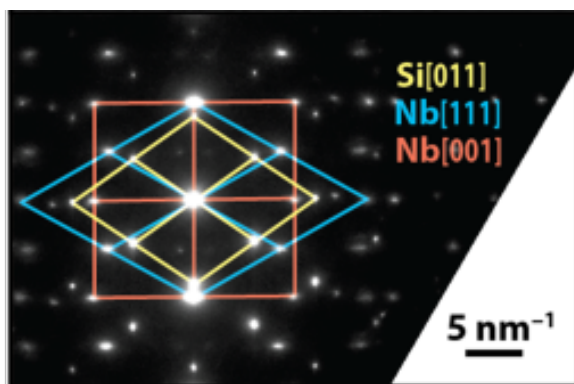


FIG. 6. (a)–(c) Microwave reflectometry comparing the lowest-loss resonators from unetched (orange), 600 s (red) and 1200 s (blue) etched chips. (a) Single-photon  $|S_{11}|$  reflectometry. The decreased peak depth at resonance shows reduced loss. (b) The resonator intrinsic loss  $\delta_{int}$  as a function of the photon number ( $n$ ), decomposed into the  $10^7$ -photon high-power loss  $\delta_{hi}$  and the single-photon loss  $\delta_{hi} + \delta_{TLS}$ , as shown by the vertical dashed lines, yielding the values shown in the inset. Etched resonators show reduced losses at all power levels. (c) The temperature-dependent  $\delta_{int}$  at  $n \approx 1$  fit to the TLS standard tunneling model (see Appendix H). The inset shows the thermal fitting results. (d) Grouped histograms correlating the resonator loss (right) and the  $\text{NbO}_x$  thickness from XPS (left) for all resonators using the method of (b). The light-colored bars show the TLS loss  $\delta_{TLS}$  and the darker bars the high-power loss  $\delta_{hi}$ , so the combined length is the measured single-photon loss. Unetched resonators (results from two different unetched “0 s” reference chips shown in blue and orange) are dominated by TLS losses, while  $\delta_{TLS}$  and  $\delta_{hi}$  are similar for etched resonators.

## 2) Evidence for Epitaxial growth of Nb on Si by magnetron sputtering



### 3) Details on Selective Etching and the Niobium Surface oxide

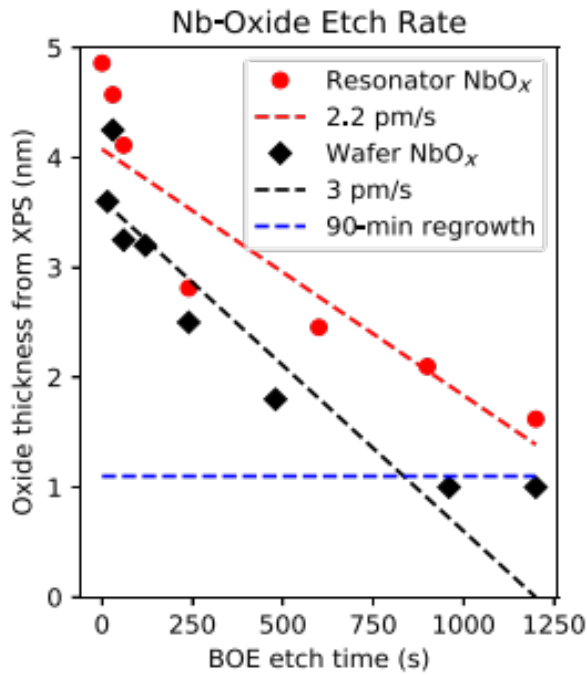


FIG. 14. The NbO<sub>x</sub> etch rate in 5:1 BOE from XPS measurements. The resonator experiments discussed in the main text are plotted in red and the data from Fig. 13 in black. The thickness variations at very short etch times reflect sample-to-sample differences in the initial oxide thickness. The resonator process oxide (red) is somewhat thicker than the process oxide simulated by plasma ashing (black).

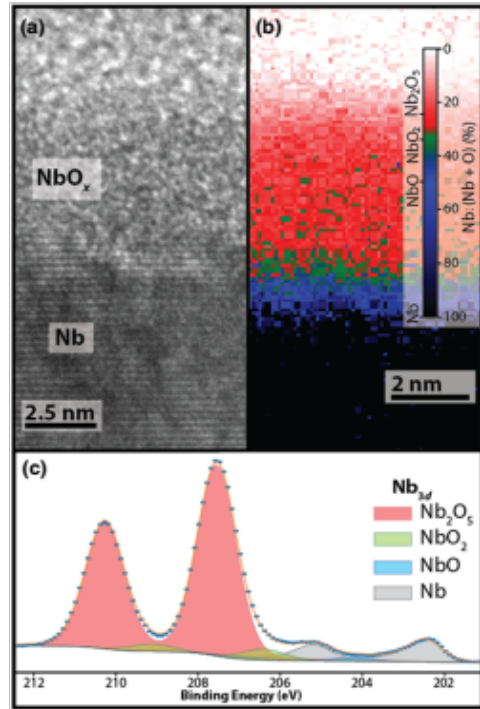


FIG. 3. The niobium metal-air (MA) interface. (a) A high-resolution TEM image showing the MA surface roughness and the approximately 4.8-nm NbO<sub>x</sub> amorphous oxide. (b) A STEM-EELS map of variations in the Nb:(Nb + O) ratio within the oxide. (c) A Nb<sub>4d</sub> XPS spectrum with peak fits to the different oxide components.

### 4) Loss Localization details

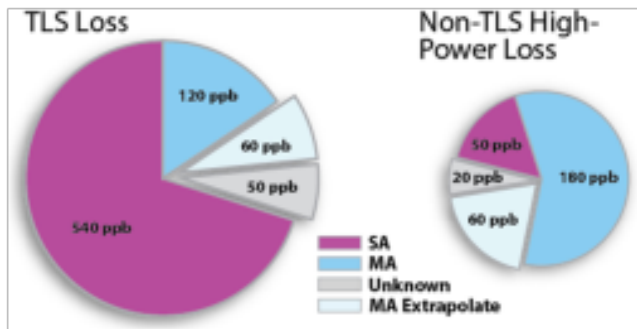


FIG. 8. The localization of 93% of both the TLS and the non-TLS loss through selective etching. The loss reduction in standard resonators due to SA etching (magenta) and MA etching (blue). The projected loss reduction from complete MA-oxide removal (light blue) extrapolated from fits in Fig. 7(c). The non-localized loss (unknown, in gray) includes contributions from the MS interface, the regrown SA oxide, and loss associated with bulk Si and Nb. The pie areas represent  $\delta_{\text{TLS}}$  and  $\delta_{\text{HP}}$  in parts per billion (ppb).

